Synthetic Nano- and Micromachines in Analytical Chemistry: Sensing, Migration, Capture, Delivery, and Separation

Wentao Duan,[1] Wei Wang,[2] Sambeeta Das,[1] Vinita Yadav,[1] Thomas E. Mallouk,[1] and Ayusman Sen[1]

[1]Department of Chemistry, The Pennsylvania State University, University Park, Pennsylvania 16802; email: tem5@psu.edu, asen@psu.edu

[2]Shenzhen Key Laboratory for Advanced Materials, School of Material Sciences and Engineering, Shenzhen Graduate School, Harbin Institute of Technology, University Town, Shenzhen 518055, China

Annu. Rev. Anal. Chem. 2015. 8:311–33

First published online as a Review in Advance on June 24, 2015

The *Annual Review of Analytical Chemistry* is online at anchem.annualreviews.org

This article's doi: 10.1146/annurev-anchem-071114-040125

Keywords

nano- and micromotors, micropumps, chemical sensing, chemotaxis, on-demand delivery

Abstract

Synthetic nano- and microscale machines move autonomously in solution or drive fluid flows by converting sources of energy into mechanical work. Their sizes are comparable to analytes (sub-nano- to microscale), and they respond to signals from each other and their surroundings, leading to emergent collective behavior. These machines can potentially enable hitherto difficult analytical applications. In this article, we review the development of different classes of synthetic nano- and micromotors and pumps and indicate their possible applications in real-time in situ chemical sensing, on-demand directional transport, cargo capture and delivery, as well as analyte isolation and separation.

1. INTRODUCTION

Machines are a fundamental part of civilization, catalyzing the evolution of human society. People have long dreamed of shrinking these machines down to the micro- or nanoscale to send them, for example, into the human body and carry out delicate in vivo operations. However, at this small scale it has been difficult to overcome the dominance of viscous and frictional forces, fluctuation from Brownian motion, and scaling laws that restrict the speed and power of microscale motors. It is only in the past decade that researchers have managed to design self-powered synthetic nano- and micromachines (1, 2) that convert chemical energy into mechanical motion. The initial discoveries have sparked tremendous interest in this emerging field (3–37), and a wide repertoire of synthetic machines that can be powered by chemical fuels (5, 12, 18, 38–47) or externally applied fields that deliver magnetic (48–56), electrical (14, 57), light (58–61), acoustic (62–64), or thermal (65–67) energy have been designed.

In analytical chemistry, many applications require real-time in situ identification and monitoring of analytes (68), as well as their on-demand transport and separation (69). For many of these tasks, shrinking the analytical tools to sizes comparable to analytes, which can range from sub-nano- (molecular) to microscale, is highly desirable. As shown in **Figure 1**, synthetic nano- and micromachines that can actively seek out, migrate toward, capture, transport, and separate analytes have been developed, potentially enabling previously difficult applications.

2. BRIEF SUMMARY ON SYNTHETIC NANO- AND MICROMACHINES

2.1. Development of Nano- and Micromotors

As with their macroscale counterparts, nano- and micromotors work by converting other forms of energy into mechanical motion. Interestingly, unlike their macroscale counterparts, synthetic nano- and micromotors typically do not have moving parts and are constrained by the time-reversal symmetry that applies in the low Reynolds number regime, the scallop theorem (37, 70, 71). This limitation requires the development of new energy transduction mechanisms to propel small-scale motors.

One common way to break time-reversal symmetry and power nano- and micromotors is to expose the motor particles to a field or gradient. Self-generated gradients allow autonomous motors to move independently from each other. Alternatively, externally applied fields can cause nonautonomous motors to move collectively in unison.

Autonomous nano- and micromotors driven by self-generated fields constitute a significant part of current motor research. Two independent early discoveries established that bimetallic metal microrods moved autonomously in hydrogen peroxide solutions (H_2O_2) (1, 2). As shown in **Figure 2*a***, the mechanism by which these motors are propelled was determined, through a series of experimental and simulation efforts, to be self-electrophoresis (42, 72–75). The essence of this mechanism is that motor particles generate concentration gradients of ions (protons, halide ions, etc.) through bipolar electrochemical reactions at the two ends of the rods. The resulting electric field induces motion of the motors themselves through electrophoresis. Other forms of motion driven by self-generated gradients have more recently been demonstrated. For example, motors driven by self-diffusiophoresis (**Figure 2*b***) are propelled by self-generated chemical concentration gradients (60, 76–78), and self-acoustophoretic motors (**Figure 2*c***) are propelled by asymmetric steady streaming of the fluid around them in an acoustic field (63, 79–81). Temperature gradients can also be used by microparticles to create motion, a mechanism referred to as self-thermophoresis (65–67).

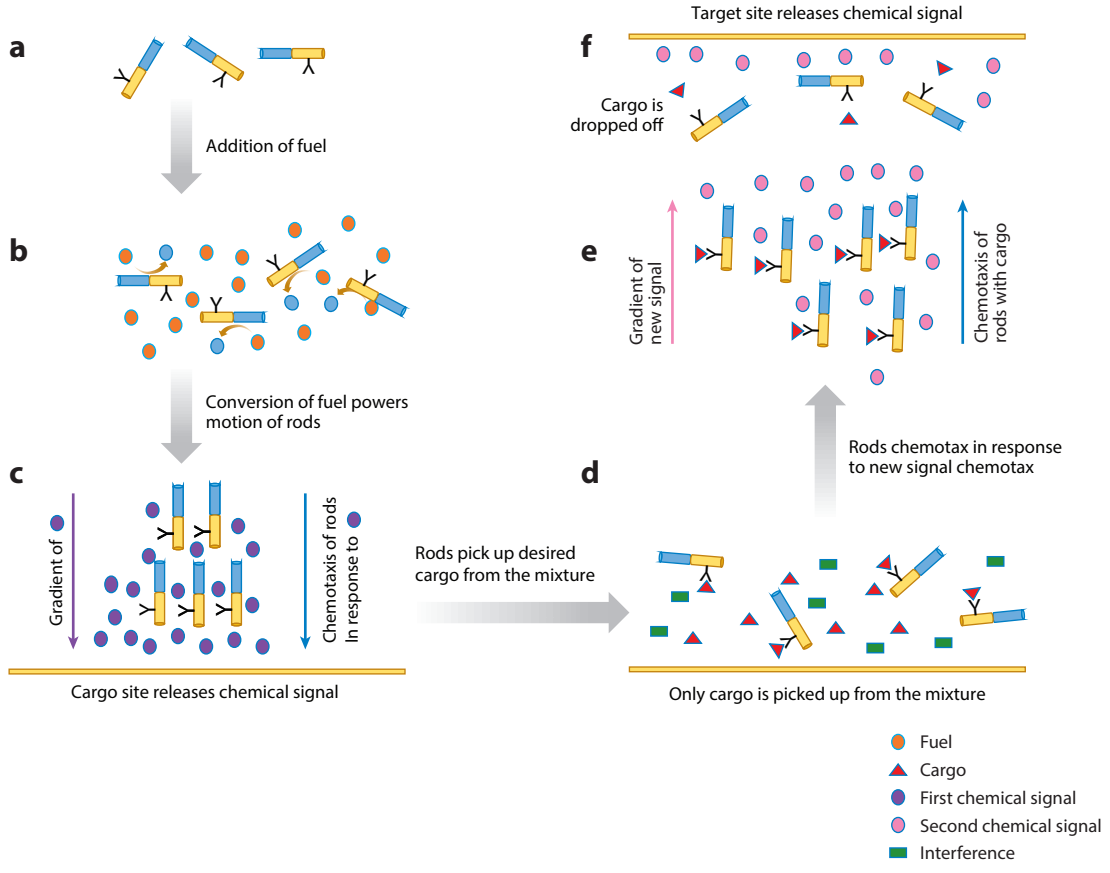

Figure 1

Illustration of the various tasks synthetic nano- and micromachines can carry out, including chemical sensing, directional migration, and cargo capture, as well as on-demand delivery and separation. An illustration of a synthetic nano- or micromachine that combines functionalities such as chemical sensing, directional migration, and cargo capture, as well as on-demand delivery and separation. (*a*,*b*) Motors move upon the addition of fuel (*orange ovals*). (*c*,*d*) The cargo site releases a chemical signal (*purple ovals*) that causes the motors to respond by migrating up the gradient of this signal to pick up the cargo (*red triangles*). (*e*,*f*) The target site releases a second chemical signal (*pink ovals*) that causes the motor to then move toward the target and deposit the cargo upon reaching the drop-off location.

Nano- and micromotors can also be driven in nonautonomous fashion by the application of external fields. For example, as shown in **Figure 2*d***, helical magnetic motors convert their body rotation into translational motion in a rotating magnetic field (48–52). Diodes (millimeter to micrometer scale) can move by converting an alternating current (AC) electric field into a local direct current (DC) field (14, 57). These externally driven nano- and micromotors, although not autonomous, have the advantage of being easy to control in terms of both speed and directionality.

Motion in another class of motors arises from the recoil of gas bubbles produced asymmetrically on the particle surface through chemical catalysis (11, 24), as shown in **Figure 2*e***. Bubble-propelled micromotors can be adapted to numerous forms, including rolled-up microtubes (27, 45), Janus microspheres (18, 82), and microtubes fabricated through electrodeposition (83–86).

Nature uses chemistry to power a myriad of biological machines and motors (87), and these have been utilized to power synthetic motors (22). As a demonstration for proof of concept, kinesin

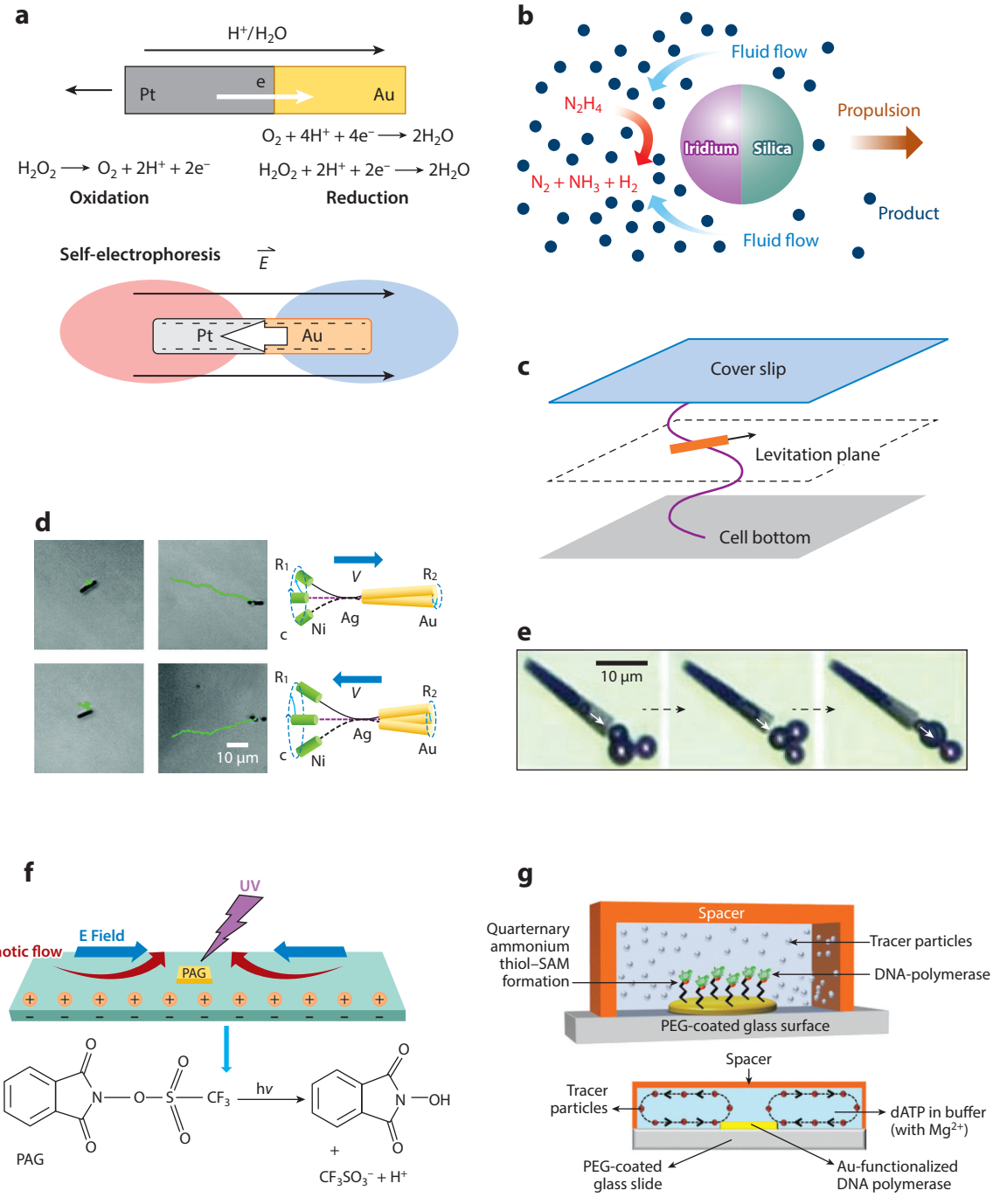

was used to propel microtubules (88), and the motor protein F1-adenosine triphosphate synthase (F1-ATPase) was used to rotate micro-nickel propellers (89). Another design is to anchor enzymes on to motors and turn over substrates to propel the motors through self-electrophoresis (40) or bubble propulsion (39, 90).

Scaling down even further, single molecule enzymes can act as autonomous motors and induce motion through substrate turnover (91, 92). Sen and coworkers (91–93) demonstrated that single enzyme molecules undergo enhanced diffusion in the presence of substrate molecules and that this diffusion increases in a substrate concentration-dependent manner. Possible mechanisms for such propulsion at the nanoscale could be nonreciprocal conformational changes (36, 94–97) or self-electrophoresis (98, 99).

2.2. Development of Micropumps

When anchored to a surface, motors transfer their mechanical energy to the surrounding fluid, directionally transporting fluid and tracer particles. The first micropumps (72, 100–102) were developed using the same principle as that of the rods that move through bipolar electrochemical reactions and involved two metals in electrical contact. With the addition of fuel, redox reactions occur at the surfaces of the metals, creating an ion gradient in the solution over the metals. The resultant electric field acts both phoretically on the charged tracer particles and osmotically on the electric double layer at the charged surface of the substrate. Tracer particles suspended in the fluid move through electrophoresis, whereas the motion of those that are close to the surface is determined by the interplay between phoresis and osmosis.

Synthetic micropumps based on self-diffusiophoresis (**Figure 2*f***) were subsequently developed (31, 103, 104). In response to external stimuli such as chemicals (31, 103) or light (104), reactions at the surface of micropumps lead to concentration gradients of ions and molecules, and thus generate fluid flows. Self-diffusiophoresis arises from two effects: electrophoresis and chemiphoresis. In electrophoresis, the difference in diffusivities of the cations and anions leads to a local electric

Figure 2

Autonomous micro- and nanomachines that are powered by different mechanisms. (*a*) Propulsion of bimetallic Pt-Au nanorods in H_2O_2 solution powered by self-electrophoresis. The electrochemical reactions at the two ends of the rod produce a gradient of protons pointing from the Pt to the Au end, and thus an electric field in the same direction. The electric field then drives the motion of the rod itself. Modified with permission from Reference 42, Copyright (2006), the American Chemical Society. (*b*) Propulsion of an iridium/silica Janus motor in N_2H_4 solution powered by self-diffusiophoresis. The chemical reaction at the active end (iridium end) produces more solute molecules, and thus induces fluid flow from the inert end (silica end). As a result, the motor is propelled with the silica end leading. Modified with permission from Reference 112, Copyright (2014), the American Chemical Society. (*c*) Propulsion of bimetallic nanorods in an acoustic field. The acoustic field levitates the motors to a certain plane where they move via self-acoustophoresis, a mechanism that is not completely understood but possibly originates from the asymmetric acoustic streaming effect. Modified with permission from Reference 79, Copyright (2012), the American Chemical Society. (*d*) Propulsion of flexible nanorods in a magnetic field; the propulsion direction can be changed by adjusting the magnetic field. Modified with permission from Reference 51, Copyright (2010), the American Chemical Society. (*e*) Propulsion of microtubes by bubble generation. Upon release of bubbles, the recoil force associated with the momentum transfer pushes the motor in the direction opposite to that of bubble release. Modified with permission from Reference 45, Copyright (2009), John Wiley and Sons. (*f*) Fluid pumping by photoacid generators in response to UV light. Upon addition of UV light, the chemical reaction produces gradients of ions near the pump, and the difference in ion diffusivities leads to local electric fields that induce electroosmotic flows near the charged surface of the substrate. Modified with permission from Reference 104, Copyright (2012), the American Chemical Society. (*g*) Fluid pumping of a DNA polymerase–modified Au pattern in response to dATP and magnesium ions. The chemical reaction produces a density gradient that drives convective fluid flow in a closed chamber. Modified with permission from Reference 93, Copyright (2014), the American Chemical Society. Abbreviations: PAG, photo-acid generator; PEG, poly(ethylene glycol); SAM, self-assembled monolayers.

field resulting in phoretic motion of tracer particles and osmotic fluid flows along the surface of the substrate. In addition, concentration gradients result in different thicknesses of double layers and thus a pressure difference along the surfaces of the particles and the pump. This causes chemiphoretic fluid flow toward areas of higher chemical concentration. The chemiphoretic effect is normally small compared to electrophoresis, and only governs fluid pumping when the cations and anions have similar diffusivities, e.g., K^+ and Cl^-.

Unlike electrophoretic micropumps that require electroconductive substrates, diffusiophoretic pumps can operate on various substrates like glass and polystyrene (104), although both systems perform poorly at high ionic strengths due to squeezed electrical double layers and attenuated diffusiophoretic flow (60, 77).

Micropumps based on density gradients (**Figure 2*g***) that are largely unaffected by high electrolyte concentrations have also been designed (105, 106). Chemical reactions at pump surfaces (64) are almost always coupled with heat generation or consumption (105). This heat flux leads to temperature gradients and thus density differences across the solution. Due to the buoyancy effect, lighter fluids move up, and denser ones settle down, which leads to convective fluid flows (106). For exothermic reactions, i.e., pumps that generate heat, fluids are pumped inward near the substrate, and for endothermic ones, outward fluid flows are generated. Density gradients can also result from density differences between reactants and products (106). Unlike the phoretic pumps discussed above, fluid velocities in density-driven pumps are influenced by the cell dimensions: for example, a sevenfold increase of velocity was observed upon doubling the cell height (105). In addition, the directions of fluid flows in density-driven systems can be reversed by inverting the pumps.

Other examples of micropumps have also been reported, including ones based on host-guest interactions (107) and bubble propulsion (108). The former generate fluid flow by uptake/release of water molecules through host-guest complexation, and the latter function by a capillary effect.

3. CHEMICAL SENSING BASED ON SYNTHETIC MACHINES

A key task in analytical chemistry is to detect the species of interest and quantify them. As discussed in Section 2, motility in synthetic nano- and micromachines depends on the presence and concentrations of specific chemical reagents in the environment, and therefore varies with changes in the reagent concentration and the presence of catalytic promoters or inhibitors (34). Thus, nano- and micromachines that can detect and quantify specific analytes have been designed (109).

3.1. Chemical Sensing with Synthetic Motors

Synthetic nano- and micromotors, when powered by chemical fuels, exhibit motility when they sense specific chemicals, e.g., hydrogen peroxide (1, 110), halogen (38), p-benzoquinone (111), and glucose (40). The motility is affected only by its local environment. Thus, variations in motility reflect changes in the local concentration of the target analyte. Detection limits are normally on the order of millimoles, although much lower levels have been reported in certain systems (112). In addition to direct observation of motion under a microscope, it has been shown that the movement of nano- and micromotors can be coupled with other phenomena, such as emission of light (113), which may lead to new detection methods for motor motion, and hence chemical sensing.

Lower detection limits can be achieved if the analyte works as a catalyst. Kagan et al. (114) demonstrated that silver ion catalyzes peroxide decomposition, and bimetallic Pt-Au rods exhibit faster motion in the presence of silver ions with concentrations as low as 1 μM (**Figure 3*a***). The increase in motor velocity has been attributed to underpotential deposition of silver onto the Pt

end. These bimetallic nanomotors also demonstrate high selectivity toward silver ions, as addition of other metal ions leads only to a drop in motor speed (114). This phenomenon has been extended to the design of motion-driven DNA-detection arrays (43). As shown in **Figure 3*b***, using a sandwich DNA hybridization assay, silver nanoparticle tags were immobilized together with DNA analyte molecules on the surface of the substrate surface. With the addition of hydrogen peroxide, dissolution of silver particles releases silver ions that promote the motility of the bimetallic nanomotors, thereby correlating the motion enhancement of nanomotors with the presence of specific DNA sequences.

Chemicals in these systems, e.g., metal ions, may exhibit matrix effects and suppress the motion of the motors, as several groups have reported (90, 115–117). By inhibiting the enzyme catalase, which is responsible for peroxide decomposition and bubble generation, contaminants in water such as mercury ions result in irreversible loss in catalase activity, and this stops the motion of enzyme-powered microengines (90). Other metal ions such as Pb^{2+} and Cd^{2+} attenuate the motion of bubble-propelled Pt microengines, with Pb^{2+} inducing the greatest decrease in motility. In the presence of 2 mM Pb^{2+} ions, the motor speed drops by approximately 80%. This allows contaminant detection and water quality monitoring by self-powered micromotors.

3.2. Chemical Sensing with Synthetic Micropumps

Synthetic micropumps are also triggered by, and hence sensitive to, certain chemical stimuli, e.g., hydrogen peroxide (72, 101, 102), hydrazine and its derivatives (100), fluoride, and magnesium ions (93, 106, 118), as well as enzyme substrates, such as urea and glucose (105). Similar to motors, the detection limit for pumps is currently on the order of millimolar concentration. Recently, pumps based on depolymerization (104, 106, 118, 119) and enzyme catalysis (93, 105) have attracted significant attention because of their ability to sense and pump in response to specific analytes. The depolymerization pumps consist of insoluble polymer films that depolymerize to release soluble monomeric products when exposed to a specific analyte, whereas the surface-anchored enzyme pumps are turned on in the presence of either the substrate, a promoter (cofactor), or a related biomarker. Both pumps are self-powered, pumping fluids and particles. In the former, depolymerization of a single polymer chain triggered by one analyte molecule leads to the release of many monomeric product molecules, resulting in considerable signal amplification and accompanying high sensitivity to the analyte. Both pumps are tunable to respond to a variety of analytes, ranging from small molecules (toxins) to enzymes (from pathogens).

The current depolymerization-powered pumps employ polymeric hydrogels or thin films [e.g., tert-butyldimethylsilyl endcapped poly(phthalaldehyde) and poly(ethyl cyanoacrylate)] as pumps. In response to chemical stimuli such as fluoride ions, hydroxide ions, and biomarkers (e.g., enzymes), depolymerization is triggered at the pump surface, and gradients of the resulting monomeric products induce fluid flows through diffusiophoresis (**Figure 3*c***). Zhang et al. (106) achieved higher sensitivity (micromolar) in such systems due to signal amplification: A specific analyte (β-D-glucuronidase, a biomarker of *Escherichia coli*) triggered fluoride release from a small molecule, which in turn caused depolymerization and fluid pumping, as shown in **Figure 3*c***. Continuing work in this area involves different amplification reactions that can provide linear or exponential responses with fast (burst release) (120) or slow (tunable) rates of amplification (121, 122).

The enzyme-powered pumps involve anchoring enzymes on the surface of gold patterns through linkers (105). These enzymes sense and turn over substrates selectively, and induce fluid flows through density gradients (**Figure 3*d***). Most of the enzyme pumps studied so far (glucose oxidase, catalase, lipase, DNA polymerase) catalyze exothermic reactions, generating heat that lowers the density of the ambient fluid and therefore pump fluid inward along the bottom surface

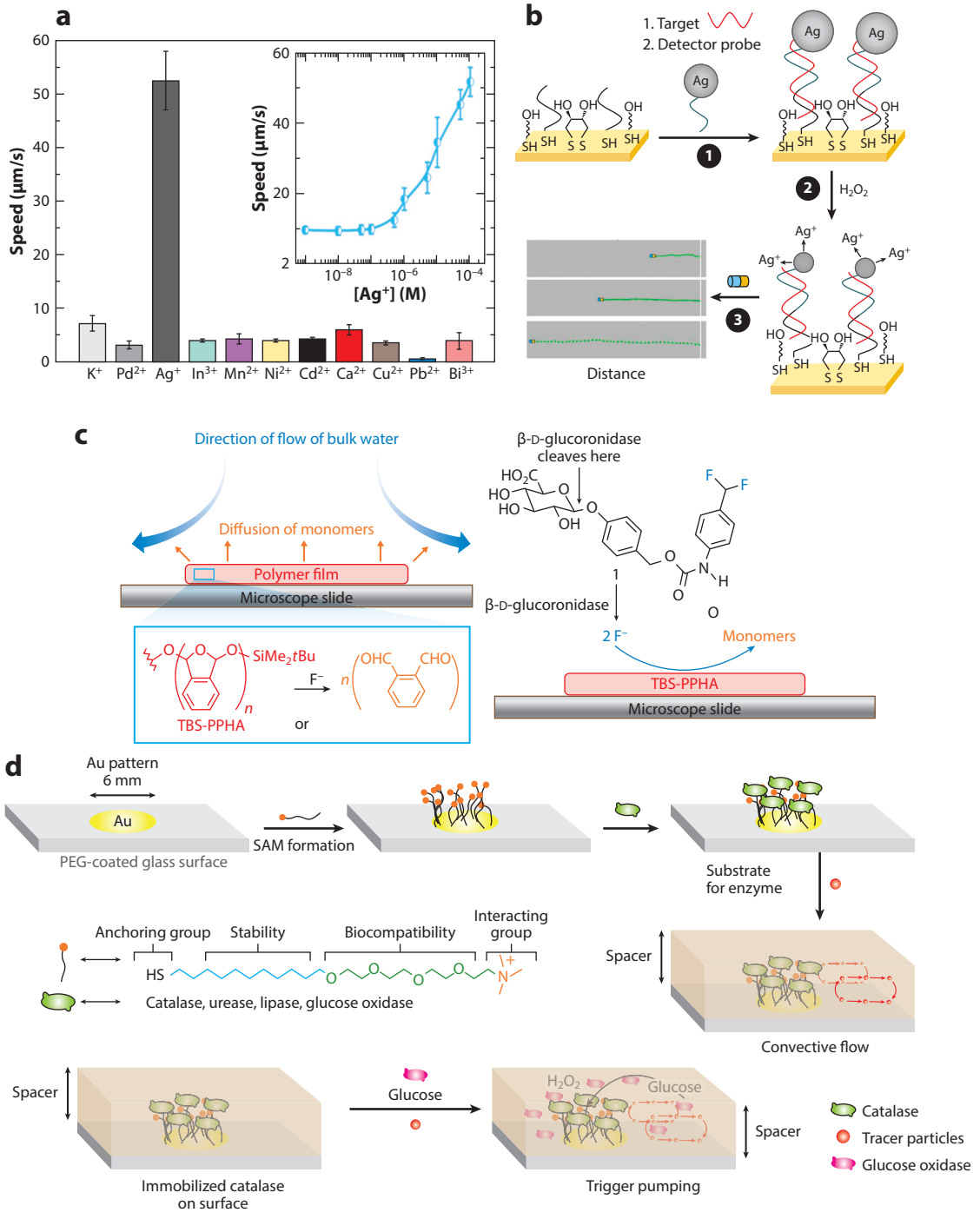

of a substrate due to buoyancy-driven convection. However urease, which hydrolyzes urea to bicarbonate and ammonium ions, increases the solution density and thus pumps outward. Enzyme promoters or cofactors (e.g., Mg^{2+}) can also trigger and regulate pumping, and thus can also be potential analytes.

3.3. Possibility of Quantitative Analysis

Besides qualitative detection, quantitative analysis is also a possibility for micromotors and pumps. Numerous systems demonstrate that the velocities of nano- and micromotors and fluid flows in micropumps have linear relationships with fuel concentrations (1, 5, 106), which makes quantitative analysis possible. However, depending on how they are fabricated, nano- and micromachines often exhibit different velocities at the same fuel concentration. Parameters such as the size and shape of synthetic machines also affect their propulsion speeds. To overcome these issues, future design of synthetic nano- and micromachines should focus on standardizing the critical parameters (34).

4. CHEMOTAXIS AND DIRECTIONAL DELIVERY

In addition to simple sensing, motors that migrate toward the source of the signal transporting molecules or particles (e.g., drugs or antigens) can be desirable. However, due to influence of Brownian motion, especially Brownian rotation, movement of synthetic motors is often randomized and lacks directionality over long time periods. One way to direct motor migration is to apply an external chemical gradient, with motors moving along or against this gradient, a phenomenon known as chemotaxis (123).

4.1. Chemotaxis

Chemotaxis has long been observed for natural systems such as bacteria (e.g., *E. coli*) (124, 125), and recently in some synthetic motors, as well as enzymes (47, 92, 93, 126, 127). The mechanism for the abiotic motors is not well understood. According to the hypothesis proposed by Hong et al. (126), when a catalytic motor experiences different diffusivities at different substrate concentrations, it will migrate toward areas of higher diffusivity. Such directional migration occurs because with higher diffusivity the motor experiences a higher average displacement so it will continue to move farther as it travels up the gradient. The hypothesis was verified experimentally by placing Pt-Au nanorods in a gradient of hydrogen peroxide: As shown in **Figure 4*a***, the population of

Figure 3

Synthetic micro- and nanomachines that are capable of chemical sensing. (*a*) Bimetallic Pt-Au nanomotors exhibit faster motion in the presence of silver ions with concentrations as low as 1 μM. Modified with permission from Reference 114, Copyright (2009), the American Chemical Society. (*b*) Design of a DNA-detection array. Silver nanoparticles are anchored to the modified surface through interaction with a detector probe and DNA analytes. Release of silver ions from the particles in response to H_2O_2 leads to faster propulsion of bimetallic nanomotors, and the concentration of the analyte can be correlated with the velocity of the motors. Modified with permission from Reference 43, Copyright (2010), Nature Publishing Group. (*c*) Design of micropumps based on depolymerization reactions that can sense fluoride ions. Higher sensitivity of analytes in such systems can be achieved by signal amplification: The analyte triggers fluoride release from a small molecule, which in turn causes depolymerization and fluid pumping. Modified with permission from Reference 106, Copyright (2012), John Wiley and Sons. (*d*) Higher sensing specificity can be achieved by enzyme-powered micropumps, which respond only to the specific substrates of the enzymes. Modified with permission from Reference 105, Copyright (2014), Nature Publishing Group. Abbreviations: PEG, poly(ethylene glycol); SAM, self-assembled monolayer; TBS-PPHA, tert-butyldimethyl-silyl end-capped poly(phthalaldehyde).

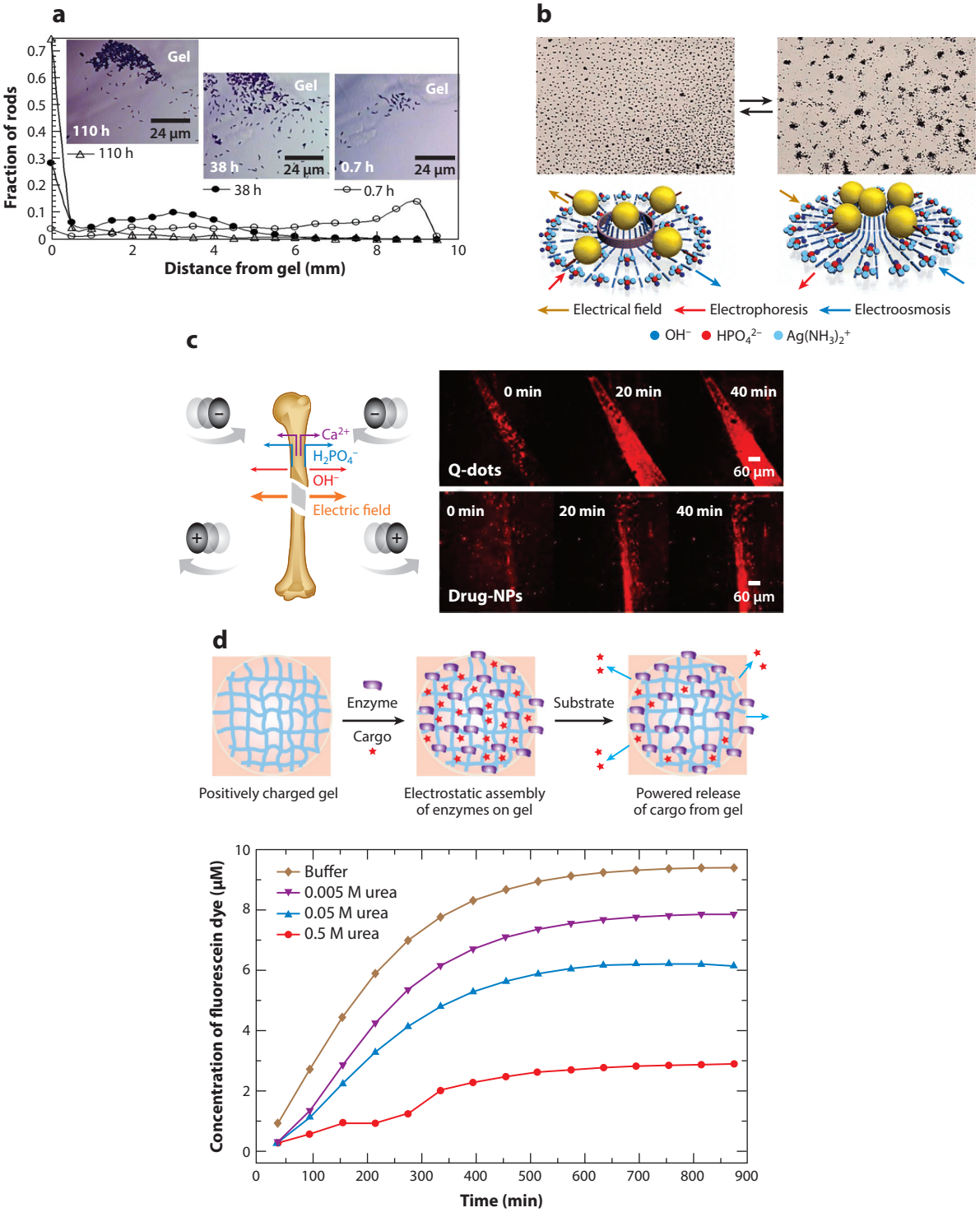

rods increases over time in regions of the highest concentration of hydrogen peroxide (where the diffusivity was highest). Similar behavior has also been discovered in polymerization-powered Janus motors (47), bubble-propelled microengines (127), and enzyme motors (92, 93).

Besides chemotaxing under external chemical signals, synthetic motors can also actively seek out chemical signals secreted by other active particles and migrate toward or away from them, referred to as a localized chemotaxis. Such interactions lead to the emergence of interesting collective behaviors such as predator-prey (60, 92), schooling (58, 60, 76, 128, 129), exclusion (77), and oscillatory motion (130). For example, in response to UV light, silver chloride microparticles produce ion gradients, and chemotax toward each other in response. Depending on the kinds of particles present and their population (128), predator-prey behavior or schooling can be observed. It is also possible to manipulate the transitions between these collective behaviors with two orthogonal input signals. As shown in **Figure 4*b***, silver orthophosphate microparticles (Ag_3PO_4) in aqueous media show transitions between "exclusion" and "schooling" (77), which are triggered by shifting the chemical equilibrium (by addition or removal of ammonia) or in response to UV light. With two inputs (ammonia and UV) and two outputs (schooling and exclusion), a logic NOR gate can be designed, opening up a new avenue for artificial intelligence with synthetic nano- and micromachines.

4.2. Directional Delivery by Micropumps

Micropumps are able to deliver fluids directionally in an axisymmetric manner. With inward and outward pumps (see Section 3.3), objects such as cargo particles are either focused at a certain area or excluded from it. Therefore, by placing micropumps in specific areas, tasks such as bone-crack repair (131) or glucose-responsive insulin release (105) can be achieved, as recently reported by the Sen group.

An inward pump, e.g., a crack in a mineral-rich material such as bone that generates ion gradient–driven electric fields (131), can be utilized for active targeting and treatment. Current methods that promote healing by delivery of a therapeutic agent to the bone operate mainly via passive diffusion (132). Mechanisms for active delivery of agents to target sites most at risk for fracture or for active degeneration remain elusive and are highly desired. Yadav et al. (131) described an active detection and repair scheme with ex vivo human bone cracks. The approach is based on the phenomenon of diffusiophoretic motion: The crack leaches out ions such as Ca^{2+}, $H_2PO_4^-$, and OH^- from freshly exposed mineral surfaces. The faster diffusivity of OH^- induces a local electric field oriented inward, toward the crack in the bone surface (i.e., the ion source). Charged moieties introduced in the system hence respond to this electric field by undergoing diffusiophoretic motion. This hypothesis was proven using charged quantum dots. Carboxylate-functionalized negatively charged quantum dots were observed to migrate

Figure 4

Synthetic micro- and nanomachines that exhibit directional migration and pumping. (*a*) Bimetallic Pt-Au nanomotors can migrate up the chemical gradient toward the source of H_2O_2 (a gel) and accumulate there. Modified with permission from Reference 126, Copyright (2007), the American Physical Society. (*b*) Micromotors can respond to each other's gradient, and collective behavior emerges. Silver orthophosphate particles can transition between two collective behaviors in response to external stimuli. Modified with permission from Reference 77, Copyright (2013), the American Chemical Society. (*c*) Release of ions from the bone crack leads to electric fields that in turn results in accumulation of quantum dots and drug nanoparticles at the crack site. Modified with permission from Reference 131, Copyright (2013), John Wiley and Sons. (*d*) Turnover of substrates by anchored enzymes on the hydrogels leads to fluid pumping that facilitates cargo release from the gel. Higher release rates can be achieved by increasing the concentrations of the substrates (i.e., urea). Modified with permission from Reference 105, Copyright (2014), Nature Publishing Group.

toward the crack, increasing the fluorescence intensity within the damage site, as shown in **Figure 4*c***. Next, the efficacy of the targeting mechanism as a drug delivery vehicle was explored by transporting biomaterials to the bone-crack site. Negatively charged, fluorescently labeled poly(lactic-coglycolic acid) (PLGA) nanoparticles containing sodium alendronate were found to migrate toward the crack and accumulate there (**Figure 4*c***). To confirm that the drug delivery vehicle delivered an active agent, an in vitro cell proliferation assay [3-(4,5-dimethylthiazol-2-yl)-5-(3-carboxymethoxyphenyl)-2-(4-sulfophenyl)-2H-tetrazolium (MTS) assay] was performed with human MG-63 cells. An increase in bone cell density was observed in cells treated with alendronate, and successful drug release was demonstrated in the PLGA nanoparticles.

Fluid flows generated by micropumps can also be employed for on-demand controlled drug release. For example, Zhang et al. (133) recently reported on a self-powered polymeric micropump based on boronate chemistry. The pump is triggered by the presence of glucose in the ambient environment and induces convective fluid flows, with pumping velocity proportional to glucose concentration. This self-powered pumping action enables the design of biocompatible, nontoxic, active delivery systems. As proof of principle, small molecule (fluorescein) release was investigated in the system using UV/Vis spectroscopy and confocal fluorescence microscopy. Additionally, Sengupta et al. (105) demonstrated active drug delivery in enzyme-powered systems (**Figure 4*d***). They anchored enzymes (i.e., urease and glucose oxidase) on quaternary ammonium-functionalized and hence positively charged hydrogel scaffolds through electrostatic interactions. The hydrogels also served as a reservoir of cargo-like dye or drug molecules. In response to substrates of the enzymes, these molecules are pumped out. The release rates increase with increasing local substrate concentrations, and are approximately an order of magnitude faster compared to purely passive diffusion. Moreover, the glucose oxidase–powered pump actively released insulin in response to ambient glucose at blood sugar level (i.e., ~5 mM), and thus functioned as a self-regulated glucose-responsive active delivery system. Future work on the topic will focus on patterning pumps that involve multienzyme cascades to enable regulation and microfluidic logic.

5. CAPTURE AND TRANSPORTATION OF ANALYTES BY SYNTHETIC MOTORS

The directional motion of nano- and micromotors enables on-demand transportation of analytes (molecules or particles). The motors can capture specific analytes via numerous mechanisms and then transport them to a specific destination guided by a magnetic field (15, 63, 85, 134, 135) or through chemotaxis. Capture of analytes can be divided into two main categories. One category commonly uses weak interactions between the nanomotor surface and the analyte, such as magnetic (**Figure 5*a***) and electrostatic forces (**Figure 5*b***), hydrophobicity/hydrophilicity (**Figure 5*c***), and hydrodynamic interactions (**Figure 5*d***). The other category instead relies on stronger interactions such as covalent bindings (**Figure 5*e***).

Magnetic interactions have been employed commonly to capture and isolate microscale cargos. For example, as shown in **Figure 5*a***, Kagan et al. (136) demonstrated Au-Pt nanomotors with a Ni segment that could capture PLGA particles that had encapsulated iron oxide cores. Similarly, Schmidt and coworkers (137) have developed catalytic Janus nanomotors that can capture and transport superparamagnetic microparticles through magnetic dipole-dipole interactions between the particle and the magnetic cap on the nanomotor. Pumera and coworkers (138) have also achieved selective isolation of paramagnetic microparticles from diamagnetic silica particles using a ferromagnetic nanomotor.

As an example of electrostatic capture (**Figure 5*b***), Sundararajan et al. (139) described a cargo-capturing nanomotor system in which a catalytic Pt-Au nanomotor with a negatively charged

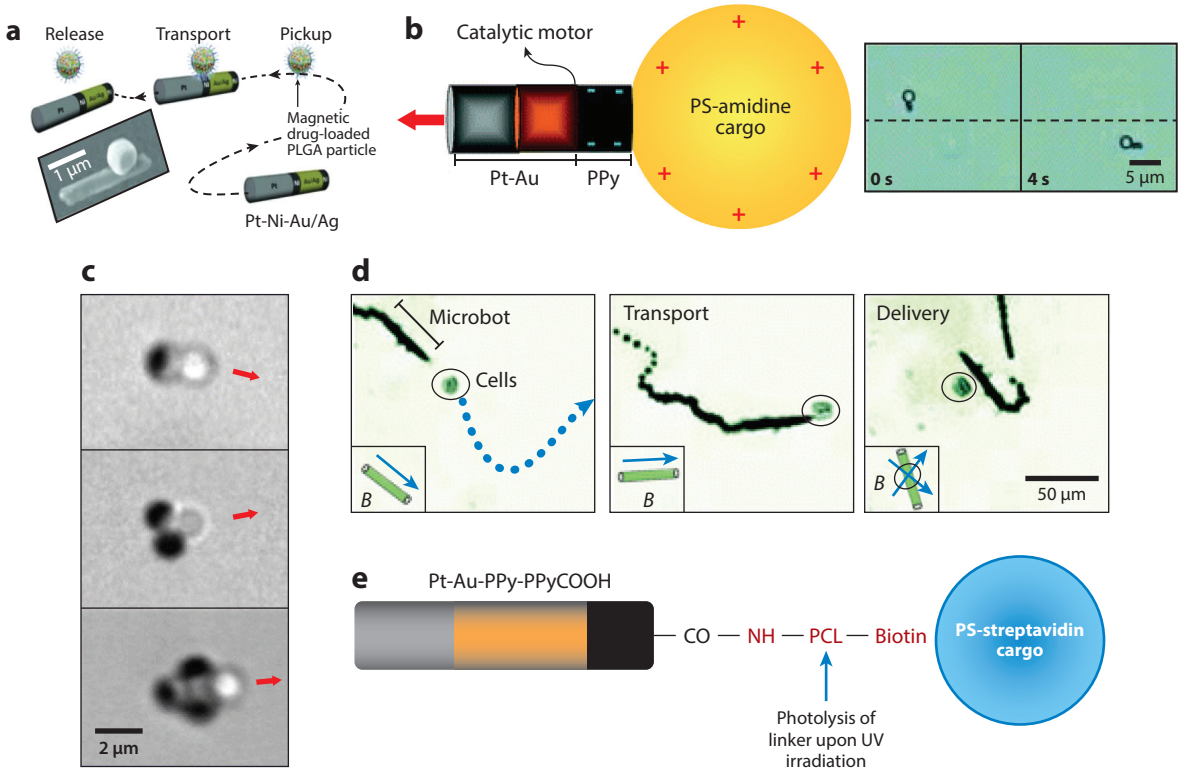

Figure 5

Synthetic micro- and nanomotors that capture cargo particles of different sizes and materials by different interactions. (*a*) Trimetallic motors (Pt-Ni-Au/Ag) with magnetic Ni segments capture particles that have an encapsulated iron oxide core. Modified with permission from Reference 136, Copyright (2010), John Wiley and Sons. (*b*) Transport of positively PS-amidine cargo through electrostatic interaction with the negatively charged PPy end of modified Pt-Au bimetallic nanomotors. Modified with permission from Reference 139, Copyright (2008), the American Chemical Society. (*c*) Interaction and assembly between a hydrophobic microsphere (*white sphere*) and Janus motors that have hydrophobic hemispheres. Modified with permission from Reference 141, Copyright (2013), the American Chemical Society. (*d*) Transport of cells by bubble-propelled microbots. Modified with permission from Reference 143, Copyright (2011), Royal Society of Chemistry. (*e*) Cargo that is attached to a motor through a photoresponsive linker can be dropped off by cleavage of the linker with UV light. Modified with permission from Reference 145, Copyright (2010), John Wiley and Sons. Abbreviations: PCL, photo-cleavable linker; PS, polystyrene.

polypyrrole (PPy) end segment was shown to capture a positively charged amidine-functionalized polystyrene microsphere (PS-amidine). In another report, the Mallouk and Sen (140) group reported on a cargo-capturing nanomotor system in which catalytic Au-Pt nanomotors were shown to pick up, one by one, generic polystyrene microspheres and assemble them into a closed-packed structure. The binding mechanism was determined through a combination of video tracking and computer simulation, to be an electrostatic interaction between the charged polystyrene particles and the electric field generated by the nanomotors.

Two hydrophobic surfaces in water can bind together, and as shown in **Figure 5*c*,** this effect was exploited by Gao et al. (141), who developed a cargo pick-up system in which a Janus micromotor with a hydrophobic hemisphere attracted and assembled hydrophobic microspheres. Similarly, the Wang (142) group has shown that microtubular motors coated with superhydrophobic

layers can capture and remove small oil droplets, demonstrating the possibilities of environmental remediation with nano- and micromotors.

Hydrodynamic interactions can also be used by nanomotors to pick up cargo, and one such example was demonstrated by Solovev et al. (135), who showed that bubble-propelled microtubes load and carry an aggregate of polystyrene microspheres through suction. Using the same suction mechanism, Sanchez et al. (143) have shown that cells can be loaded and manipulated by tubular micromotors (**Figure 5*d***), especially with the help of external magnetic fields.

Mechanical forces can also be used to achieve cargo transport by nanomotors. Nelson and coworkers (53) showed that, in an external magnetic field, a rotating Ni nanowire near a flat surface can penetrate a nearby polystyrene microsphere and form a doublet. Through such mechanical coupling, the polystyrene particle can be manipulated and transported. Subsequent offloading was achieved by reversing the direction of the applied magnetic field. In another example, Schmidt and coworkers (135) showed that microtubular motors can transport and assemble magnetic microplates through mechanical pushing.

Micromotors with specially designed structures can also capture and deliver cargo through geometric locking, and this was clearly demonstrated by two magnetically propelled micromotor systems developed by the Nelson (144) group. In one experiment, 3D e-beam lithography was used to fabricate cage-like micromotors that allowed cells to grow inside them (144). These motors were subsequently activated and propelled using an external rotating magnetic field, and the cells within the motor cage were transported during the process. In another example, helical micromachines with a microholder were fabricated through the same 3D lithographic technique. Cargo particles were shown to be captured by these holders (50).

Nano- and micromotors can also capture analytes through covalent binding between the functional groups on the nanomotor surface and the analyte. For example, Sundararajan et al. (145) functionalized the Au end of a Au-Pt catalytic nanomotor with a self-assembled monolayer of biotin-terminated disulfide and achieved cargo pickup of streptavidin-functionalized polystyrene microspheres through a biotin-streptavidin interaction, as shown in **Figure 5*e***. The same group later used a photocleavable linker to connect the PPy segment of a Pt-Au catalytic nanomotor with a polystyrene microsphere using the same biotin-streptavidin interaction (145). In a series of experiments, the Wang group has achieved pickup and transport of nucleic acids (146), proteins (147), cancer cells (148), and bacteria (149) with microtubular motors functionalized with ss-DNA, aptamers, antibodies, and lectins, respectively. Similar mechanisms can also be applied to other nanomotor systems, such as those driven by ultrasound (80). These experiments have demonstrated the capabilities of functionalized nano- and micromotors (or so-called micromachines) to isolate biological samples on the fly.

The number of cargo particles being delivered by an active micromotor and their sizes have a significant impact on the performance and behavior of the micromotor. Empirically, increasing the size of the cargo will increase the drag force exerted on the cargo-motor aggregate, causing the motor to slow down. This has been confirmed by multiple groups in experiments conducted with various types of micromotors. For example, one early report by Sen and coworkers (139) showed that the speed of a catalytic Au-Pt nanomotor carrying one polystyrene microsphere decreased from 7.4 μm/s to 5.9 μm/s and further to 3.9 μm/s when the radius of the sphere increased from 0 (no cargo) to 0.38 μm and to 1.05 μm. Wang and coworkers (136) showed a similar trend in their experiments with catalytic nanoshuttles carrying PLGA particles via magnetic interactions. In this case, a nanomotor with an original speed of 16 μm/s traveled at speeds of 13.5, 9.7, and 6.3 μm/s when carrying cargo particles of 0.8-, 1.3-, and 2.0-μm diameter, respectively. Solovev et al. (135) reported that bubble-propelled nanomotors pushing magnetic nanoplates showed an inverse exponential speed decrease as the plate surface area increased. Due to the same hydrodynamic

effect, the speed of micromotors will decrease as they carry more and more cargo particles, as demonstrated in numerous reports (135, 140, 141).

6. SEPARATION AND ISOLATION

By capturing and transporting specific analytes, synthetic micromachines can separate and isolate them from other materials and enrich them in an area of interest. Micromotors have been used for the separation/isolation of a variety of analytes, including bacteria (149), cancer cells (148), nucleic acids (146), proteins (147), and paramagnetic particles (138).

Self-propelled objects can also be separated from their inert counterparts by exploiting the catalytic and chemotactic abilities of the former. Most current separation techniques at the nano- or microscale use continuous flow devices, which often require an external force field. In addition, these techniques separate species based on differences in their physical properties such as shape (150), density (151), or charge (152). This presents a problem in multicomponent sorting, given the physical difference between particles is often not enough for efficient separation (151). This problem may be overcome by separating species on the basis of their self-powered propulsion and chemotaxis. The powered motion of active particles enables them to migrate against external flows and applied forces (153). As shown in **Figure 6*a***, Volpe et al. (154) demonstrated a possible route for separation of active Au/silica Janus particles from particles that undergo only Brownian motion. Under light illumination, the Janus particles self-propel based on a self-diffusiophoresis mechanism, and propulsion velocities increase with light intensity. In the presence of an array of periodically arranged obstacles, active Janus swimmers can steer away from, and even move perpendicular to, an externally applied force, whereas Brownian swimmers merely follow the force lines.

Another separation route is based on chemotaxis of active swimmers. As discussed in Section 4, chemotaxis is a phenomenon that is only associated with active matter systems. Thus, by applying a concentration gradient of fuel, active swimmers can be separated from their inactive Brownian counterparts, given only the former will migrate up the gradient, as shown in **Figure 6*b*,*c***. The Sen (155) group recently demonstrated that enzymes migrate up the gradients of their substrates (**Figure 6*c***). On the basis of this affinity, it is possible to separate enzyme molecules of similar sizes and isoelectric points, which is unprecedented in the literature. By placing a mixture of two enzymes in one channel, and the substrate for one in the other, it is possible to isolate the catalytically active biomolecules from the corresponding inactive ones (155). A similar system was reported by Baraban et al. (127), in which active microengines were isolated from inert microtubes by migrating toward the other channel that contained their fuel (hydrogen peroxide). In principle, the technique of chemotactic separation can be used to separate active catalysts from their less active or inactive counterparts in the presence of their respective substrates and should, therefore, find wide applicability.

7. PERSPECTIVES

As discussed above, a broad variety of synthetic nano- and micromachines have been designed to accomplish tasks ranging from sensing and capture to delivery and separations. The reaction-induced enhanced diffusion of catalytic particles (e.g., enzymes), as well as catalytic fluid pumping, can overcome analyte transport limitations in highly sensitive assays. Assays that use nano- and micrometer-scale particles as platforms are currently limited in sensitivity due to slow mass transport of the analyte to the sensor. For analyses at the femtomolar level, nanoscale sensors can require hours to days to collect only a few molecules (156). Active transport attenuates this problem,

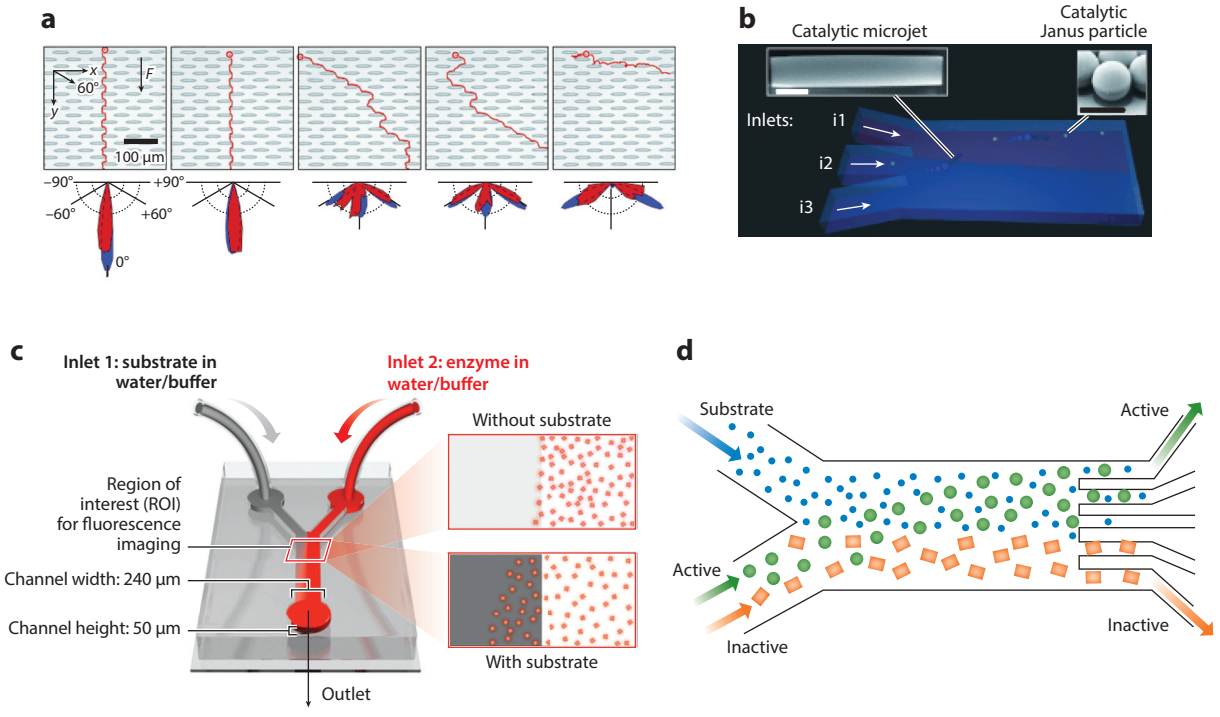

Figure 6

Separation of micro- and nanomachines. (*a*) Isolation of micromotors with patterns by an applied force in the *y*-direction. Active particles can migrate in the *x*-direction, whereas inert ones would only follow the external force. Modified with permission from Reference 154, Copyright (2011), Royal Society of Chemistry. (*b*) Catalytic Janus particles can migrate toward other channels that contain their fuels. Modified with permission from Reference 127, Copyright (2013), John Wiley and Sons. (*c*) Enzymes chemotax toward channels that contain their respective substrates. Modified with permission from Reference 92, Copyright (2013), the American Chemical Society. (*d*) Such chemotaxis phenomena can be employed to separate enzymes by placing a mixture of two enzymes in one channel and the substrate for one in the other. Modified with permission from Reference 155, Copyright (2014), the American Chemical Society.

and detection of trace analytes above the background can be achieved in a much shorter time. Swarms of chemically or acoustically powered micromotors can cover millimeter distances within seconds, collecting analyte molecules as cargo and then dropping them off at a specific location for sensing. Alternatively, self-powered pumps can actively transport the analyte containing fluid to the sensor for rapid detection. In addition, because no external power source is required, sensors can be deployed in remote locations and can lie dormant until triggered by specific analytes. Motion-based sensing also constitutes a novel way to direct particle movement toward specific targets, while allowing them to sample a large region of fluid space by powered diffusive motion.

The observation of collective behavior such as predator-prey allows the fabrication of particles with different functionalities that can act collectively, thereby simplifying design of intelligent assemblies. In general, access to rationally designed dynamic materials that are capable of remodeling themselves and transforming their environment will (*a*) minimize waste (they will change their function and purpose rather than being single-use), (*b*) improve performance (they will continuously refine their structures to optimize performance), and (*c*) accomplish tasks collectively and emergently (like a colony of ants), which a single constituent element (like a single ant) cannot perform. By making these dynamic materials self-powered, they will also be

capable of exploring and responding to their environment (sensor and cargo-release applications) without being tethered to a single power source or location.

Finally, microfluidic pumps that turn on and off in response to specific signals (see **Figure 3**) can function as smart devices that can spatially separate particles or molecular analytes and route them to the sensor elements of microfluidic devices. Because enzyme-based pumps can be coupled together chemically with a high degree of specificity (i.e., one pump can generate a substrate or inhibitor for the next one in the series), it may be possible to make chemically powered lab-on-a-chip devices that incorporate logic and signal amplification. Chemically powered logical operations (**Figure 4*b***) and amplification (**Figure 3*a–c***) have already been demonstrated in nonenzymatic systems of nanomotors and pumps. Together these active systems hold great promise for sensing of trace molecules in chemical, biochemical, and clinical applications.

SUMMARY POINTS

1. Living systems serve as the blueprint for many of the synthetic nano- and micromotor designs. The ultimate goal is to make synthetic motors that mimic the functionalities of their biological analogs.
2. Synthetic nano- and micromachines can be powered by a myriad of mechanisms, including self-electrophoresis, self-diffusiophoresis, self-acoustophoresis, density gradients, host-guest interactions, and bubble propulsion.
3. The motility of synthetic nano- and micromotors as well as fluid pumping by micropumps are strongly influenced by the presence and concentrations of specific ions and chemicals in the environment and thus can be used as sensing probes for these analytes.
4. Nano- and micromotors move directionally in response to gradients of specific ions or chemicals. The biomimetic chemotaxis gives rise to such collective phenomena as schooling, exclusion, predator-prey, and oscillatory motion.
5. The chemotactic response can be employed for the capture, transport, and delivery of cargo by synthetic motors. Micropumps can similarly transport fluid and particles to a given location in response to specific chemical triggers.
6. Chemotaxis can be employed to separate catalytic nano- and micromotors from their less active or inert counterparts in the presence of their respective substrates.
7. Active transport by synthetic motors and pumps allows them to collect and concentrate analytes at specific locations for rapid sensing.

DISCLOSURE STATEMENT

The authors are not aware of any affiliations, memberships, funding, or financial holdings that might be perceived as affecting the objectivity of this review.

ACKNOWLEDGMENTS

We thank the many coworkers and collaborators who have contributed to our work over the past decade. This research has been conducted in the Penn State Center for Nanoscale Science, a Materials Research Science and Engineering Center supported by the National Science Foundation under grant DMR-0820404. We also thank the Defense Threat Reduction Agency (HDTRA1-13-1-0039).

LITERATURE CITED

1. Paxton WF, Kistler KC, Olmeda CC, Sen A, St. Angelo SK, et al. 2004. Catalytic nanomotors: autonomous movement of striped nanorods. *J. Am. Chem. Soc.* 126:13424–31
2. Fournier-Bidoz S, Arsenault AC, Manners I, Ozin GA. 2005. Synthetic self-propelled nanorotors. *Chem. Commun.* 2005:441–43
3. Ozin GA, Manners I, Fournier-Bidoz S, Arsenault A. 2005. Dream nanomachines. *Adv. Mater.* 17:3011–18
4. Paxton WF, Sundararajan S, Mallouk TE, Sen A. 2006. Chemical locomotion. *Angew. Chem. Int. Ed.* 45:5420–29
5. Howse JR, Jones RAL, Ryan AJ, Gough T, Vafabakhsh R, Golestanian R. 2007. Self-motile colloidal particles: from directed propulsion to random walk. *Phys. Rev. Lett.* 99:048102
6. Mallouk TE, Sen A. 2009. Powering nanorobots. *Sci. Am.* 300:72–77
7. Sen A, Ibele M, Hong Y, Velegol D. 2009. Chemo and phototactic nano/microbots. *Faraday Discuss.* 143:15–27
8. Gibbs JG, Fragnito NA, Zhao Y. 2010. Asymmetric Pt/Au coated catalytic micromotors fabricated by dynamic shadowing growth. *Appl. Phys. Lett.* 97:253107
9. Ke H, Ye S, Carroll RL, Showalter K. 2010. Motion analysis of self-propelled Pt-silica particles in hydrogen peroxide solutions. *J. Phys. Chem. A* 114:5462–67
10. Mirkovic T, Zacharia NS, Scholes GD, Ozin GA. 2010. Nanolocomotion—catalytic nanomotors and nanorotors. *Small* 6:159–67
11. Loget G, Kuhn A. 2011. Electric field-induced chemical locomotion of conducting objects. *Nat. Commun.* 2:535
12. Golestanian R, Liverpool TB, Ajdari A. 2005. Propulsion of a molecular machine by asymmetric distribution of reaction products. *Phys. Rev. Lett.* 94:220801
13. Hess H. 2006. Self-assembly driven by molecular motors. *Soft Matter* 2:669–77
14. Chang ST, Paunov VN, Petsev DN, Velev OD. 2007. Remotely powered self-propelling particles and micropumps based on miniature diodes. *Nat. Mater.* 6:235–40
15. Dhar P, Cao YY, Kline T, Pal P, Swayne C, et al. 2007. Autonomously moving local nanoprobes in heterogeneous magnetic fields. *J. Phys. Chem. C* 111:3607–13
16. Chang ST, Beaumont E, Petsev DN, Velev OD. 2008. Remotely powered distributed microfluidic pumps and mixers based on miniature diodes. *Lab Chip* 8:117–24
17. Golestanian R, Ajdari A. 2008. Mechanical response of a small swimmer driven by conformational transitions. *Phys. Rev. Lett.* 100:038101
18. Gibbs JG, Zhao YP. 2009. Autonomously motile catalytic nanomotors by bubble propulsion. *Appl. Phys. Lett.* 94:163104–3
19. Gibbs JG, Zhao YP. 2009. Design and characterization of rotational multicomponent catalytic nanomotors. *Small* 5:2304–8
20. Sánchez S, Pumera M. 2009. Nanorobots: the ultimate wireless self-propelled sensing and actuating devices. *Chem. Asian J.* 4:1402–10
21. Tao YG, Kapral R. 2009. Dynamics of chemically powered nanodimer motors subject to an external force. *J. Chem. Phys.* 131:024113
22. Wang J. 2009. Can man-made nanomachines compete with nature biomotors? *ACS Nano* 3:4–9
23. Ebbens SJ, Howse JR. 2010. In pursuit of propulsion at the nanoscale. *Soft Matter* 6:726–38
24. Loget G, Kuhn A. 2010. Propulsion of microobjects by dynamic bipolar self-regeneration. *J. Am. Chem. Soc.* 132:15918–19
25. Ramaswamy S. 2010. The mechanics and statistics of active matter. *Annu. Rev. Condens. Matter Phys.* 1:323–45
26. Wheat PM, Marine NA, Moran JL, Posner JD. 2010. Rapid fabrication of bimetallic spherical motors. *Langmuir* 26:13052–55
27. Mei Y, Solovev AA, Sanchez S, Schmidt OG. 2011. Rolled-up nanotech on polymers: from basic perception to self-propelled catalytic microengines. *Chem. Soc. Rev.* 40:2109–19

28. Miño G, Mallouk TE, Darnige T, Hoyos M, Dauchet J, et al. 2011. Enhanced diffusion due to active swimmers at a solid surface. *Phys. Rev. Lett.* 106:048102
29. Gao W, Sattayasamitsathit S, Wang J. 2012. Catalytically propelled micro-/nanomotors: How fast can they move? *Chem. Rec.* 12:224–31
30. Masoud H, Bingham BI, Alexeev A. 2012. Designing maneuverable micro-swimmers actuated by responsive gel. *Soft Matter* 8:8944–51
31. Reinmuller A, Oguz EC, Messina R, Lowen H, Schope HJ, Palberg T. 2012. Colloidal crystallization in the quasi-two-dimensional induced by electrolyte gradients. *J. Chem. Phys.* 136:164505–10
32. Sengupta S, Ibele ME, Sen A. 2012. Fantastic voyage: designing self-powered nanorobots. *Angew. Chem. Int. Ed.* 51:8434–45
33. Solovev AA, Xi W, Gracias DH, Harazim SM, Deneke C, et al. 2012. Self-propelled nanotools. *ACS Nano* 6:1751–56
34. Wang W, Duan W, Ahmed S, Mallouk TE, Sen A. 2013. Small power: autonomous nano- and micromotors propelled by self-generated gradients. *Nano Today* 8:531–54
35. Soler L, Sanchez S. 2014. Catalytic nanomotors for environmental monitoring and water remediation. *Nanoscale* 6: 7175–82
36. Sakaue T, Kapral R, Mikhailov AS. 2010. Nanoscale swimmers: hydrodynamic interactions and propulsion of molecular machines. *Eur. Phys. J. B* 75:381–87
37. Kapral R. 2013. Perspective: nanomotors without moving parts that propel themselves in solution. *J. Chem. Phys.* 138:020901
38. Liu R, Sen A. 2011. Autonomous nanomotor based on copper–platinum segmented nanobattery. *J. Am. Chem. Soc.* 133:20064–67
39. Pantarotto D, Browne WR, Feringa BL. 2008. Autonomous propulsion of carbon nanotubes powered by a multienzyme ensemble. *Chem. Commun.* 2008:1533–35
40. Mano N, Heller A. 2005. Bioelectrochemical propulsion. *J. Am. Chem. Soc.* 127:11574–75
41. Kline TR, Paxton WF, Mallouk TE, Sen A. 2005. Catalytic nanomotors: remote-controlled autonomous movement of striped metallic nanorods. *Angew. Chem. Int. Ed.* 44:744–46
42. Paxton WF, Baker PT, Kline TR, Wang Y, Mallouk TE, Sen A. 2006. Catalytically induced electrokinetics for motors and micropumps. *J. Am. Chem. Soc.* 128:14881–88
43. Wu J, Balasubramanian S, Kagan D, Manesh KM, Campuzano S, Wang J. 2010. Motion-based DNA detection using catalytic nanomotors. *Nat. Commun.* 1:36
44. Stock C, Heureux N, Browne WR, Feringa BL. 2008. Autonomous movement of silica and glass microobjects based on a catalytic molecular propulsion System. *Chem. Eur. J.* 14:3146–53
45. Solovev AA, Mei Y, Bermúdez Ureña E, Huang G, Schmidt OG. 2009. Catalytic microtubular jet engines self-propelled by accumulated gas bubbles. *Small* 5:1688–92
46. Gao W, Sattayasamitsathit S, Orozco J, Wang J. 2011. Highly efficient catalytic microengines: template electrosynthesis of polyaniline/platinum microtubes. *J. Am. Chem. Soc.* 133:11862–64
47. Pavlick RA, Sengupta S, McFadden T, Zhang H, Sen A. 2011. A polymerization-powered motor. *Angew. Chem. Int. Ed.* 50:9374–77
48. Zhang L, Abbott JJ, Dong L, Peyer KE, Kratochvil BE, et al. 2009. Characterizing the swimming properties of artificial bacterial flagella. *Nano Lett.* 9:3663–67
49. Ghosh A, Fischer P. 2009. Controlled propulsion of artificial magnetic nanostructured propellers. *Nano Lett.* 9:2243–45
50. Tottori S, Zhang L, Qiu F, Krawczyk KK, Franco-Obregon A, Nelson BJ. 2012. Magnetic helical micromachines: fabrication, controlled swimming, and cargo transport. *Adv. Mater.* 24:811–16
51. Gao W, Sattayasamitsathit S, Manesh KM, Weihs D, Wang J. 2010. Magnetically powered flexible metal nanowire motors. *J. Am. Chem. Soc.* 132:14403–5
52. Dreyfus R, Baudry J, Roper ML, Fermigier M, Stone HA, Bibette J. 2005. Microscopic artificial swimmers. *Nature* 437:862–65
53. Zhang L, Petit T, Lu Y, Kratochvil BE, Peyer KE, et al. 2010. Controlled propulsion and cargo transport of rotating nickel nanowires near a patterned solid surface. *ACS Nano* 4:6228–34
54. Tierno P, Golestanian R, Pagonabarraga I, Sagués F. 2008. Magnetically actuated colloidal microswimmers. *J. Phys. Chem. B* 112:16525–28

55. Masoud H, Alexeev A. 2010. Modeling magnetic microcapsules that crawl in microchannels. *Soft Matter* 6:794–99
56. Fischer P, Ghosh A. 2011. Magnetically actuated propulsion at low Reynolds numbers: towards nanoscale control. *Nanoscale* 3:557–63
57. Calvo-Marzal P, Sattayasamitsathit S, Balasubramanian S, Windmiller JR, Dao C, Wang J. 2010. Propulsion of nanowire diodes. *Chem. Commun.* 46:1623–24
58. Hong Y, Diaz M, Córdova-Figueroa UM, Sen A. 2010. Light-driven titanium-dioxide-based reversible microfireworks and micromotor/micropump systems. *Adv. Funct. Mater.* 20:1568–76
59. Liu M, Zentgraf T, Liu Y, Bartal G, Zhang X. 2010. Light-driven nanoscale plasmonic motors. *Nat. Nanotechnol.* 5:570–73
60. Ibele M, Mallouk TE, Sen A. 2009. Schooling behavior of light-powered autonomous micromotors in water. *Angew. Chem. Int. Ed.* 48:3308–12
61. Abid J-P, Frigoli M, Pansu R, Szeftel J, Zyss J, et al. 2011. Light-driven directed motion of azobenzene-coated polymer nanoparticles in an aqueous medium. *Langmuir* 27:7967–71
62. Wang W, Li S, Mair L, Ahmed S, Huang TJ, Mallouk TE. 2014. Acoustic propulsion of nanorod motors inside living cells. *Angew. Chem. Int. Ed.* 126:3265–68
63. Ahmed S, Wang W, Mair LO, Fraleigh RD, Li S, et al. 2013. Steering acoustically propelled nanowire motors toward cells in a biologically compatible environment using magnetic fields. *Langmuir* 29:16113–18
64. Kagan D, Benchimol MJ, Claussen JC, Chuluun-Erdene E, Esener S, Wang J. 2012. Acoustic droplet vaporization and propulsion of perfluorocarbon-loaded microbullets for targeted tissue penetration and deformation. *Angew. Chem. Int. Ed.* 51:7519–22
65. Jiang HR, Yoshinaga N, Sano M. 2010. Active motion of a Janus particle by self-thermophoresis in a defocused laser beam. *Phys. Rev. Lett.* 105:268302
66. Baraban L, Streubel R, Makarov D, Han L, Karnaushenko D, et al. 2012. Fuel-free locomotion of Janus motors: magnetically induced thermophoresis. *ACS Nano* 7:1360–67
67. Qian B, Montiel D, Bregulla A, Cichos F, Yang H. 2013. Harnessing thermal fluctuations for purposeful activities: the manipulation of single micro-swimmers by adaptive photon nudging. *Chem. Sci.* 4:1420–29
68. Murray R. 2010. Challenges in environmental analytical chemistry. *Anal. Chem.* 82:1569–69
69. Pappas D, Wang K. 2007. Cellular separations: a review of new challenges in analytical chemistry. *Anal. Chim. Acta* 601:26–35
70. Abbott JJ, Peyer KE, Lagomarsino MC, Zhang L, Dong L, et al. 2009. How should microrobots swim? *Int. J. Robot. Res.* 28:1434–47
71. Purcell EM. 1977. Life at low Reynolds number. *Am. J. Phys.* 45:3–11
72. Kline TR, Iwata J, Lammert PE, Mallouk TE, Sen A, Velegol D. 2006. Catalytically driven colloidal patterning and transport. *J. Phys. Chem. B* 110:24513–21
73. Wang Y, Hernandez RM, Bartlett DJ, Bingham JM, Kline TR, et al. 2006. Bipolar electrochemical mechanism for the propulsion of catalytic nanomotors in hydrogen peroxide solutions. *Langmuir* 22:10451–56
74. Moran JL, Posner JD. 2011. Electrokinetic locomotion due to reaction-induced charge auto-electrophoresis. *J. Fluid Mech.* 680:31–66
75. Yariv E. 2010. Electrokinetic self-propulsion by inhomogeneous surface kinetics. *Proc. R. Soc. A* 467:1645–64
76. Kagan D, Balasubramanian S, Wang J. 2011. Chemically triggered swarming of gold microparticles. *Angew. Chem. Int. Ed.* 50:503–6
77. Duan W, Liu R, Sen A. 2013. Transition between collective behaviors of micromotors in response to different stimuli. *J. Am. Chem. Soc.* 135:1280–83
78. Ebbens S, Tu MH, Howse JR, Golestanian R. 2012. Size dependence of the propulsion velocity for catalytic Janus-sphere swimmers. *Phys. Rev. E* 85:020401(R)
79. Wang W, Castro LA, Hoyos M, Mallouk TE. 2012. Autonomous motion of metallic microrods propelled by ultrasound. *ACS Nano* 6:6122–32
80. Garcia-Gradilla V, Orozco J, Sattayasamitsathit S, Soto F, Kuralay F, et al. 2013. Functionalized ultrasound-propelled magnetically guided nanomotors: toward practical biomedical applications. *ACS Nano* 7:9232–40

81. Nadal F, Lauga E. 2014. Asymmetric steady streaming as a mechanism for acoustic propulsion of rigid bodies. *Phys. Fluids* 26:082001
82. Wilson DA, Nolte RJM, van Hest JCM. 2012. Autonomous movement of platinum-loaded stomatocytes. *Nat. Chem.* 4:268–74
83. Manesh KM, Cardona M, Yuan R, Clark M, Kagan D, et al. 2010. Template-assisted fabrication of salt-independent catalytic tubular microengines. *ACS Nano* 4:1799–804
84. Gao W, Manesh KM, Hua J, Sattayasamitsathit S, Wang J. 2011. Hybrid nanomotor: a catalytically/magnetically powered adaptive nanowire swimmer. *Small* 7:2047–51
85. Zhao G, Pumera M. 2012. Magnetotactic artificial self-propelled nanojets. *Langmuir* 29:7411–15
86. Zhao G, Ambrosi A, Pumera M. 2013. Self-propelled nanojets via template electrodeposition. *Nanoscale* 5:1319–24
87. Mirkovic T, Zacharia NS, Scholes GD, Ozin GA. 2010. Fuel for thought: chemically powered nanomotors out-swim nature's flagellated bacteria. *ACS Nano* 4:1782–89
88. Brunner C, Wahnes C, Vogel V. 2007. Cargo pick-up from engineered loading stations by kinesin driven molecular shuttles. *Lab Chip* 7:1263–71
89. Soong RK, Bachand GD, Neves HP, Olkhovets AG, Craighead HG, Montemagno CD. 2000. Powering an inorganic nanodevice with a biomolecular motor. *Science* 290:1555–58
90. Orozco J, García-Gradilla V, D'Agostino M, Gao W, Cortés A, Wang J. 2012. Artificial enzyme-powered microfish for water-quality testing. *ACS Nano* 7:818–24
91. Muddana HS, Sengupta S, Mallouk TE, Sen A, Butler PJ. 2010. Substrate catalysis enhances single-enzyme diffusion. *J. Am. Chem. Soc.* 132:2110–11
92. Sengupta S, Dey KK, Muddana HS, Tabouillot T, Ibele ME, et al. 2013. Enzyme molecules as nanomotors. *J. Am. Chem. Soc.* 135:1406–14
93. Sengupta S, Spiering MM, Dey KK, Duan W, Patra D, et al. 2014. DNA polymerase as a molecular motor and pump. *ACS Nano* 8:2410–18
94. Lauga E. 2011. Enhanced diffusion by reciprocal swimming. *Phys. Rev. Lett.* 106:178101
95. Cressman A, Togashi Y, Mikhailov AS, Kapral R. 2008. Mesoscale modeling of molecular machines: Cyclic dynamics and hydrodynamical fluctuations. *Phys. Rev. E* 77:050901
96. Iima M, Mikhailov AS. 2009. Propulsion hydrodynamics of a butterfly micro-swimmer. *EPL* (*Europhysics Letters*) 85:44001
97. Golestanian R. 2010. Synthetic mechanochemical molecular swimmer. *Phys. Rev. Lett.* 105:018103
98. Lee T-C, Alarcón-Correa M, Miksch C, Hahn K, Gibbs JG, Fischer P. 2014. Self-propelling nanomotors in the presence of strong Brownian forces. *Nano Lett.* 14:2407–12
99. Peter HC, Raymond K. 2014. Ångström-scale chemically powered motors. *EPL* 106:30004
100. Ibele ME, Wang Y, Kline TR, Mallouk TE, Sen A. 2007. Hydrazine fuels for bimetallic catalytic microfluidic pumping. *J. Am. Chem. Soc.* 129:7762–63
101. Kline TR, Paxton WF, Wang Y, Velegol D, Mallouk TE, Sen A. 2005. Catalytic micropumps: microscopic convective fluid flow and pattern formation. *J. Am. Chem. Soc.* 127:17150–51
102. Jun I-K, Hess H. 2010. A biomimetic, self-pumping membrane. *Adv. Mater.* 22:4823–25
103. McDermott JJ, Kar A, Daher M, Klara S, Wang G, et al. 2012. Self-generated diffusioosmotic flows from calcium carbonate micropumps. *Langmuir* 28:15491–97
104. Yadav V, Zhang H, Pavlick R, Sen A. 2012. Triggered "on/off" micropumps and colloidal photodiode. *J. Am. Chem. Soc.* 134:15688–91
105. Sengupta S, Patra D, Rivera IO, Agrawal A, Dey KK, et al. 2014. Self-powered enzyme micropumps. *Nat. Chem.* 6:415–22
106. Zhang H, Yeung K, Robbins JS, Pavlick RA, Wu M, et al. 2012. Self-powered microscale pumps based on analyte-initiated depolymerization reactions. *Angew. Chem. Int. Ed.* 51:2400–4
107. Patra D, Zhang H, Sengupta S, Sen A. 2013. Dual stimuli-responsive, rechargeable micropumps *via* "host-guest" interactions. *ACS Nano* 7:7674–79
108. Solovev AA, Sanchez S, Mei Y, Schmidt OG. 2011. Tunable catalytic tubular micro-pumps operating at low concentrations of hydrogen peroxide. *Phys. Chem. Chem. Phys.* 13:10131–35
109. Bunea A-I, Pavel I-A, David S, Gáspár S. 2015. Sensing based on the motion of enzyme-modified nanorods. *Biosens. Bioelectron.* 67:42–48

110. Demirok UK, Laocharoensuk R, Manesh KM, Wang J. 2008. Ultrafast catalytic alloy nanomotors. *Angew. Chem. Int. Ed.* 47:9349–51
111. Yoshizumi Y, Date Y, Ohkubo K, Yokokawa M, Suzuki H. 2013. *Bimetallic micromotor autonomously movable in biofuels*. Presented at Micro Electro Mech. Sys. (MEMS), Inst. Electr. Electron. Eng. (IEEE), 26th, Seoul, S. Korea
112. Gao W, Pei A, Dong R, Wang J. 2014. Catalytic iridium-based Janus micromotors powered by ultralow levels of chemical fuels. *J. Am. Chem. Soc.* 136:2276–79
113. Sentic M, Loget G, Manojlovic D, Kuhn A, Sojic N. 2012. Light-emitting electrochemical "swimmers." *Angew. Chem. Int. Ed.* 51:11284–88
114. Kagan D, Calvo-Marzal P, Balasubramanian S, Sattayasamitsathit S, Manesh KM, et al. 2009. Chemical sensing based on catalytic nanomotors: motion-based detection of trace silver. *J. Am. Chem. Soc.* 131:12082–83
115. Zhao G, Sanchez S, Schmidt OG, Pumera M. 2013. Poisoning of bubble propelled catalytic micromotors: the chemical environment matters. *Nanoscale* 5:2909–14
116. Zhao G, Wang H, Khezri B, Webster RD, Pumera M. 2013. Influence of real-world environments on the motion of catalytic bubble-propelled micromotors. *Lab Chip* 13:2937–41
117. Moo JGS, Wang H, Zhao G, Pumera M. 2014. Biomimetic artificial inorganic enzyme-free self-propelled microfish robot for selective detection of Pb^{2+} in water. *Chem. Eur. J.* 20:4292–96
118. DiLauro AM, Zhang H, Baker MS, Wong F, Sen A, Phillips ST. 2013. Accessibility of responsive end-caps in films composed of stimuli-responsive, depolymerizable poly(phthalaldehydes). *Macromolecules* 46:7257–65
119. Baker MS, Yadav V, Sen A, Phillips ST. 2013. A self-powered polymeric material that responds autonomously and continuously to fleeting stimuli. *Angew. Chem. Int. Ed.* 52:10295–99
120. DiLauro AM, Abbaspourrad A, Weitz DA, Phillips ST. 2013. Stimuli-responsive core–shell microcapsules with tunable rates of release by using a depolymerizable poly(phthalaldehyde) membrane. *Macromolecules* 46:3309–13
121. Schmid KM, Jensen L, Phillips ST. 2012. A self-immolative spacer that enables tunable controlled release of phenols under neutral conditions. *J. Org. Chem.* 77:4363–74
122. Nuñez SA, Yeung K, Fox NS, Phillips ST. 2011. A structurally simple self-immolative reagent that provides three distinct, simultaneous responses per detection event. *J. Org. Chem.* 76:10099–113
123. Van Haastert PJ, Devreotes PN. 2004. Chemotaxis: signalling the way forward. *Nat. Rev. Mol. Cell Biol.* 5:626–34
124. Macnab RM, Koshland D. 1972. The gradient-sensing mechanism in bacterial chemotaxis. *Proc. Natl. Acad. Sci. USA* 69:2509–12
125. Berg HC, Brown DA. 1972. Chemotaxis in *Escherichia coli* analysed by three-dimensional tracking. *Nature* 239:500–4
126. Hong Y, Blackman NMK, Kopp ND, Sen A, Velegol D. 2007. Chemotaxis of nonbiological colloidal rods. *Phys. Rev. Lett.* 99:178103
127. Baraban L, Harazim SM, Sanchez S, Schmidt OG. 2013. Chemotactic behavior of catalytic motors in microfluidic channels. *Angew. Chem. Int. Ed.* 52:5552–56
128. Duan W, Ibele M, Liu R, Sen A. 2012. Motion analysis of light-powered autonomous silver chloride nanomotors. *Eur. Phys. J. E* 35:77–84
129. Solovev AA, Sanchez S, Schmidt OG. 2013. Collective behaviour of self-propelled catalytic micromotors. *Nanoscale* 5:1284–93
130. Ibele ME, Lammert PE, Crespi VH, Sen A. 2010. Emergent, collective oscillations of self-mobile particles and patterned surfaces under redox conditions. *ACS Nano* 4:4845–51
131. Yadav V, Freeman JD, Grinstaff M, Sen A. 2013. Bone-crack detection, targeting, and repair using ion gradients. *Angew. Chem. Int. Ed.* 52:10997–1001
132. Arns S, Gibe R, Moreau A, Monzur Morshed M, Young RN. 2012. Design and synthesis of novel bone-targeting dual-action pro-drugs for the treatment and reversal of osteoporosis. *Biorg. Med. Chem.* 20:2131–40
133. Zhang H, Duan W, Lu M, Zhao X, Shklyaev S, et al. 2014. Self-powered glucose-responsive micropumps. *ACS Nano* 8:8537–42

134. Chaturvedi N, Hong Y, Sen A, Velegol D. 2010. Magnetic enhancement of phototaxing catalytic motors. *Langmuir* 26:6308–13
135. Solovev AA, Sanchez S, Pumera M, Mei YF, Schmidt OG. 2010. Magnetic control of tubular catalytic microbots for the transport, assembly, and delivery of micro-objects. *Adv. Funct. Mater.* 20:2430–35
136. Kagan D, Laocharoensuk R, Zimmerman M, Clawson C, Balasubramanian S, et al. 2010. Rapid delivery of drug carriers propelled and navigated by catalytic nanoshuttles. *Small* 6:2741–47
137. Baraban L, Makarov D, Streubel R, Monch I, Grimm D, et al. 2012. Catalytic Janus motors on microfluidic chip: deterministic motion for targeted cargo delivery. *ACS Nano* 6:3383–89
138. Zhao G, Wang H, Sanchez S, Schmidt OG, Pumera M. 2013. Artificial micro-Cinderella based on self-propelled micromagnets for the active separation of paramagnetic particles. *Chem. Commun.* 49:5147–49
139. Sundararajan S, Lammert PE, Zudans AW, Crespi VH, Sen A. 2008. Catalytic motors for transport of colloidal cargo. *Nano Lett.* 8:1271–76
140. Wang W, Duan W, Sen A, Mallouk TE. 2013. Catalytically powered dynamic assembly of rod-shaped nanomotors and passive tracer particles. *Proc. Natl. Acad. Sci. USA* 110:17744–49
141. Gao W, Pei A, Feng X, Hennessy C, Wang J. 2013. Organized self-assembly of Janus micromotors with hydrophobic hemispheres. *J. Am. Chem. Soc.* 135:998–1001
142. Guix M, Orozco J, Garcia M, Gao W, Sattayasamitsathit S, et al. 2012. Superhydrophobic alkanethiol-coated microsubmarines for effective removal of oil. *ACS Nano* 6:4445–51
143. Sanchez S, Solovev AA, Schulze S, Schmidt OG. 2011. Controlled manipulation of multiple cells using catalytic microbots. *Chem. Commun.* 47:698–700
144. Kim S, Qiu F, Kim S, Ghanbari A, Moon C, et al. 2013. Fabrication and characterization of magnetic microrobots for three-dimensional cell culture and targeted transportation. *Adv. Mater.* 25:5863–68
145. Sundararajan S, Sengupta S, Ibele ME, Sen A. 2010. Drop-off of colloidal cargo transported by catalytic Pt–Au nanomotors via photochemical stimuli. *Small* 6:1479–82
146. Kagan D, Campuzano S, Balasubramanian S, Kuralay F, Flechsig G-U, Wang J. 2011. Functionalized micromachines for selective and rapid isolation of nucleic acid targets from complex samples. *Nano Lett.* 11:2083–87
147. Orozco J, Campuzano S, Kagan D, Zhou M, Gao W, Wang J. 2011. Dynamic isolation and unloading of target proteins by aptamer-modified microtransporters. *Anal. Chem.* 83:7962–69
148. Balasubramanian S, Kagan D, Jack Hu C-M, Campuzano S, Lobo-Castañon MJ, et al. 2011. Micromachine-enabled capture and isolation of cancer cells in complex media. *Angew. Chem. Int. Ed.* 50:4161–64
149. Campuzano S, Orozco J, Kagan D, Guix M, Gao W, et al. 2011. Bacterial isolation by lectin-modified microengines. *Nano Lett.* 12:396–401
150. Masaeli M, Sollier E, Amini H, Mao W, Camacho K, et al. 2012. Continuous inertial focusing and separation of particles by shape. *Phys. Rev. X* 2:031017
151. Ito Y, Shinomiya K. 2001. A new continuous-flow cell separation method based on cell density: principle, apparatus, and preliminary application to separation of human buffy coat. *J. Clin. Apheresis* 16:186–91
152. Schägger H, von Jagow G. 1987. Tricine-sodium dodecyl sulfate-polyacrylamide gel electrophoresis for the separation of proteins in the range from 1 to 100 kDa. *Anal. Biochem.* 166:368–79
153. Ozin GA. 2013. Channel crossing by a catalytic nanomotor. *Chemcatchem* 5:2798–801
154. Volpe G, Buttinoni I, Vogt D, Kummerer H-J, Bechinger C. 2011. Microswimmers in patterned environments. *Soft Matter* 7:8810–15
155. Dey KK, Das S, Poyton MF, Sengupta S, Cremer PS, Sen A. 2014. Chemotactic separation of enzymes. *ACS Nano* 8:11941–49
156. Sheehan PE, Whitman LJ. 2005. Detection limits for nanoscale biosensors. *Nano Lett.* 5:803–7

Annual Review of
Analytical Chemistry

Volume 8, 2015

Contents

Indexes

Errata

An online log of corrections to *Annual Review of Analytical Chemistry* articles may be found at http://www.annualreviews.org/errata/anchem